coatings

Article

Model and Algorithm for a Rotor-Bearing System Considering Journal Misalignment

Zhiming Zhao *, Junjie Ma, Qi Liu and Peiji Yang

College of Mechanical and Electrical Engineering, Xi'an Campus, Shaanxi University of Science and Technology, Xi'an 710021, China; 220512096@sust.edu.cn (J.M.); 210511003@sust.edu.cn (Q.L.); 4664@sust.edu.cn (P.Y.)
* Correspondence: zhaozhiming@sust.edu.cn

Abstract: Disturbances caused as a result of the misalignment and axial motion of the journal affect the characteristics of the rotor-bearing system. This paper aims to propose an algorithm for the theoretical analysis of a rotor-bearing system that considers these disturbances. A theoretical model for a journal bearing considering disturbances is given. The dynamic equations for a rigid rotor-bearing system are introduced. A detailed algorithm that can simultaneously solve the rotor-dynamic equations and the Reynolds equation is proposed. The static performance, such as the bearing attitude angle and the fluid film pressure, are given, and dynamic characteristics such as the nonlinear dynamic responses and the axial orbits of a rigid rotor-bearing system are presented. The hydrodynamic effect of the bearing is enhanced by the axial disturbance. Disturbances in the circumferential and radial directions lead to variations in the fluid film thickness distribution in the axial direction and the offset of the fluid film pressure distribution in the axial direction. When these disturbances work together, the variation trend is more obvious and affects the capacity and dynamic characteristics of the bearing. When the L/D value of the bearing increases, the clearance between the journal and the bearing decreases rapidly. When the value reaches a certain limit, contact and collision might occur. The theoretical analysis method and the algorithm proposed for a rotor-bearing system considering several disturbances could enhance the design level for a bearing and rotor-bearing system.

Keywords: disturbance; journal bearing; fluid film pressure; rotor-bearing system; nonlinear response

check for updates

Citation: Zhao, Z.; Ma, J.; Liu, Q.; Yang, P. Model and Algorithm for a Rotor-Bearing System Considering Journal Misalignment. *Coatings* **2024**, *14*, 48. https://doi.org/10.3390/coatings14010048

Academic Editor: Jose Luis Viesca

Received: 20 November 2023
Revised: 21 December 2023
Accepted: 21 December 2023
Published: 28 December 2023

1. Introduction

Journal bearings are widely used in rotating machinery such as steam turbines, gas turbines, water turbines, and compressors, among others. The static and dynamic characteristics of the journal bearing affect the dynamic behaviors of the rotor-bearing system significantly. When working conditions such as the working parameters of both the bearing and the rotor vary, the characteristics of the bearing vary accordingly. Many studies concentrate on these topics.

The disturbances caused by serious working conditions contribute many variations to the bearing performance and the influence of dynamic behaviors on the rotor-bearing system. Some possible explanations for the disturbances include the effects of transmission parts, load variation, the Morton effect, deformation, a rotor with a large unbalanced mass, and the structure of the single bearing support. When the rotating machinery is used on ships or vehicles, disturbances such as axial motion and misalignment might occur. These disturbances can cause the fluid film characteristics of the bearing to vary, which might influence the dynamic behavior of the rotor-bearing system.

Many studies have focused on plain journal bearings, tilting-pad bearings [1], four-pocket bearings [2], and air bearings [3] without considering the effects of rotor misalignment. The characteristics of journal bearings and rolling bearings considering this misalignment were discussed mainly through theoretical analysis. The influences of turbulent effects [4,5], textured surfaces [6,7], and THD (thermo-hydrodynamic) [8–10] were considered. The characteristics of rolling bearings considering an inner ring misalignment were also researched [11]. For a new kind of MR (Magnetorheological) journal bearing, misalignment and surface irregularities were considered [12]. Misalignment also has significant effects on the thrust bearings [5,13]. An experiment and numerical research was carried out in order to explain mixed lubrication when considering misalignment [14].

The linear [15] and nonlinear [16–18] effects on the bearing characteristics caused by rotor disturbances were also researched. The axial motion [19–21] was also taken into consideration. The effects of misalignment of the rotor-bearing system on the fault diagnosis was also a hot topic [22,23]. However, there is less research concentrating on the comprehensive effects, including axial motion and radial and circumferential disturbances of the rotor. There is a lack of discussion of the dynamic characteristics of rotor-bearing systems [24] due to the complex theoretical analysis.

This paper aims to explain the influences of several disturbances on the journal bearings and the rotor-bearing system and to enhance the design level for a bearing and rotor-bearing system. In order to explain the influences of several disturbances on the journal bearings and the rotor-bearing system, especially for the bearings with a larger length-to-diameter ratio, detailed work related to the theoretical modeling and simulation analysis of a rigid rotor-bearing system is proposed. The theoretical models of both the bearing and the rotor-bearing system are given in Section 2, and detailed explanations of the algorithms are also presented in this section. Section 3 presents the simulation results of the bearing and rotor-bearing system with a detailed discussion. The brief conclusions are shown in Section 4.

2. Model and Algorithm

2.1. Journal Disturbances

Disturbances can affect the capability and dynamic characteristics of journal bearings. Therefore, the journal bearing model with disturbances considered should be given more attention. A rotor-bearing system with certain disturbances is shown in Figure 1. When the journal is disturbed, it may rotate around the *x*-coordinate axis, rotate around the *z*-coordinate axis, or translate along the *z*-coordinate axis. When the disturbances appear, the axial center will move near a balance point. Assuming that $O'(e_{0x}, e_{0z})$ is the initial position of the mass center of the rotor, the coordinates' relationship to the balance point can be expressed by the following:

$$\begin{cases} e_{0x} = e_0 \sin\ \theta_0 \\ e_{0y} = e_0 \cos\ \theta_0 \\ \tan\ \theta_0 = e_{0x}/e_{0y} \end{cases} \tag{1}$$

where e_0 is the distance between O and O′, while θ_0 is the angle between line $\overline{OO'}$ and the *x*-axis positive direction.

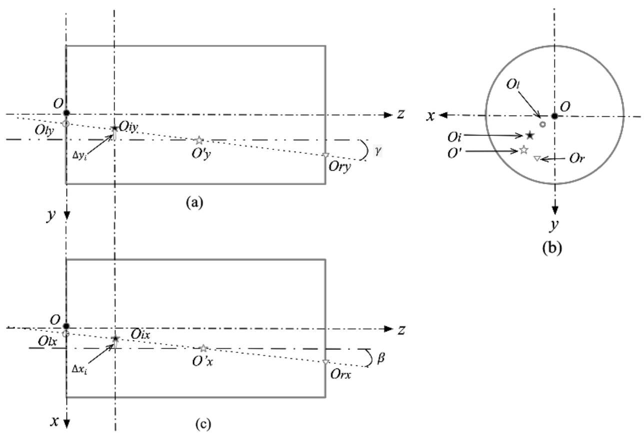

Figure 1. Schematic diagram of journal disturbances. (**a**) Front view; (**b**) side view; (**c**) top view.

Assume that $O_i(e_{ix}, e_{iy})$ is the i-th point on the rotor axis related to the z-coordinate. The journal rotates around the x-coordinate axis and the y-coordinate axis, which can be denoted by γ and β, respectively. Then, e_{iy} and e_{ix} can be written as follows:

$$\begin{cases} e_{iy} = e_{0y} \pm \Delta y_i \\ e_{ix} = e_{0xi} \pm \Delta x_i \end{cases} \tag{2}$$

where Δy_i and Δx_i can be expressed as

$$\Delta y_i = \begin{cases} \left(\frac{L}{2} - z_i\right)\tan\gamma \approx \left(\frac{L}{2} - z_i\right)\gamma, & z_i \in [0, \frac{L}{2}] \\ \left(-\frac{L}{2} + z_i\right)\tan\gamma \approx \left(-\frac{L}{2} + z_i\right)\gamma, & z_i \in [\frac{L}{2}, L] \end{cases} \tag{3}$$

$$\Delta x_i = \begin{cases} \left(\frac{L}{2} - z_i\right)\tan\beta \approx \left(\frac{L}{2} - z_i\right)\beta, & z_i \in [0, \frac{L}{2}) \\ \left(-\frac{L}{2} + z_i\right)\tan\beta \approx \left(-\frac{L}{2} + z_i\right)\beta, & z_i \in [\frac{L}{2}, L] \end{cases} \tag{4}$$

So, the new balance position, $O_i(e_{ix}, e_{iy})$, is written as

$$e_i = \sqrt{{e_{ix}}^2 + {e_{iy}}^2} = \sqrt{\left[e_0 \sin\theta_0 + \left(-\frac{L}{2} + z_i\right)\beta\right]^2 + \left[e_0 \cos\theta_0 + \left(-\frac{L}{2} + z_i\right)\gamma\right]^2} \tag{5}$$

$$\tan\theta_i = \frac{e_{ix}}{e_{iy}} = \frac{e_0 \sin\theta_0 + \left(-\frac{L}{2} + z_i\right)\beta}{e_0 \cos\theta_0 + \left(-\frac{L}{2} + z_i\right)\gamma} \tag{6}$$

where e_i is the distance between O and O', while θ_0 is the angle between $\overline{OO_i}$ and an *x*-axis positive direction.

Furthermore, O_l and O_r are the intersection points between the rotor axis and the left and right end faces of the bearings. The position can be found in Figure 1.

2.2. Model of Journal Bearing

A hydrodynamic bearing considering the journal disturbances is presented in Figure 2a. The dimensionless fluid film thickness, considering journal disturbances, is written as follows:

$$H = 1 + e_i \cos(\theta - \theta_i)/c \tag{7}$$

where c is the difference between the bearing radius and the shaft radius, also known as the radial clearance of the journal bearing.

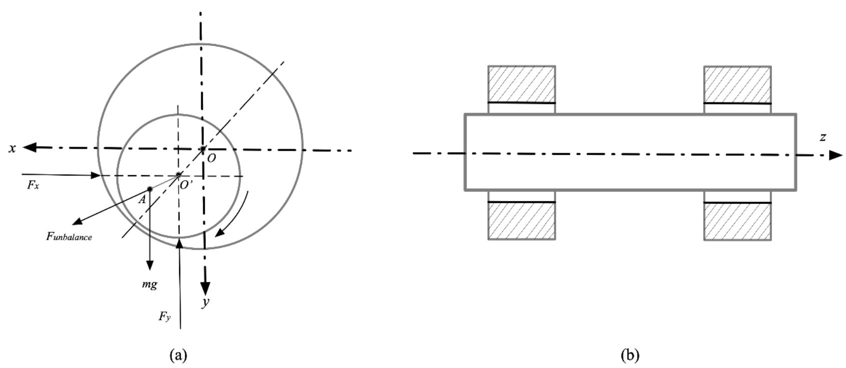

Figure 2. Schematic diagram of a hydrodynamic bearing and a rigid rotor system: (**a**) bearing; (**b**) rotor-bearing system.

Without taking into consideration the viscosity variation with respect to temperature and turbulence, the hydrodynamic journal bearing is described by the following:

$$\frac{\partial}{\partial x}\left(\frac{h^3}{\mu}\frac{\partial p}{\partial x}\right)+\frac{\partial}{\partial z}\left(\frac{h^3}{\mu}\frac{\partial p}{\partial z}\right)=6\,\overline{U}\frac{\partial h}{\partial x}+6\,\overline{W}\frac{\partial h}{\partial z}+12\,\overline{V} \tag{8}$$

where *x* and *z* are the coordinates of the rotor rotating direction and axial direction, respectively, and h, p, μ, $\overline{U}$, $\overline{W}$, and $\overline{V}$ are the thickness of the fluid film, the distribution of pressure, the viscosity of the fluid, the normal velocity, the axial velocity, and the tangential velocity of the rotor, respectively.

2.3. Model of Rotor-Bearing System

A rigid rotor with an unbalanced mass is taken as an example to analyze the dynamic characteristics shown in Figure 2b. The rotor is supported by the same two journal bearings. The rotor mass is 2 m and the unbalance radius is $\xi=\overline{O'A}$. The values F_x and F_y are the nonlinear fluid film forces. Due to the nonlinear characteristics of the fluid film forces and the rotor unbalance at higher rotor eccentricity, the nonlinear effects of the rotor-bearing system should be considered.

The rotor is affected by the fluid film forces at both sides, as shown in Figure 2a. The dynamic model of the rigid rotor-bearing system can be expressed as

$$\begin{cases} 2m\ddot{x}=-2F_x+F_{unbalance}\sin\omega t \\ 2m\ddot{y}=-2F_y+2W+F_{unbalance}\cos\omega t \end{cases} \tag{9}$$

where $F_{unbalance}=2\xi m\omega^2$, x and y are the responses of the journal along the x- and y-directions, and $2W=2$ mg is the rotor weight. The model can be rewritten as

$$\begin{cases} m\ddot{x}=-F_x+\xi m\omega^2\sin\omega t \\ m\ddot{y}=-F_y+W+\xi m\omega^2\cos\omega t \end{cases} \tag{10}$$

which is expressed with the state equation and output equation as follows:

$$\sum:\begin{cases} \begin{Bmatrix} \dot{Y}_1 \\ \dot{Y}_2 \\ \dot{Y}_3 \\ \dot{Y}_4 \end{Bmatrix}=\begin{cases} Y_2 \\ \frac{1}{m}\left(-F_x+\xi m\omega^2\sin\omega t\right) \\ Y_4 \\ \frac{1}{m}\left(-F_y+W+\xi m\omega^2\cos\omega t\right) \end{cases} \\ \begin{Bmatrix} x \\ y \end{Bmatrix}=\begin{Bmatrix} Y_1 \\ Y_3 \end{Bmatrix} \end{cases} \tag{11}$$

The boundary conditions of these equations are as follows:

$$\begin{cases} Y_1(0)=x_0 \\ Y_2(0)=0 \\ Y_3(0)=y_0 \\ Y_4(0)=0 \end{cases} \tag{12}$$

where ($Y_1(0)$, $Y_3(0)$) is the initial equilibrium position of the journal bearing and $Y_2(0)$ and $Y_4(0)$ are the initial velocities along the x-direction and y-direction of the mass center of the journal bearing.

2.4. Algorithm

The Reynolds equation is solved using the finite difference method. The procedures of calculating the bearing with journal disturbances can be concluded in two steps: (1) Input the initial parameters of the bearing to solve the steady Reynolds equation; then, the equilibrium position is obtained, which can be expressed with the eccentricity ratio and the attitude angle. (2) Using the eccentricity ratio and the attitude angle obtained in the previous step, the Reynolds equation considering the disturbances is solved to obtain the fluid film pressure, fluid film thickness, and the capability of the bearing. The details can be found in Figure 3.

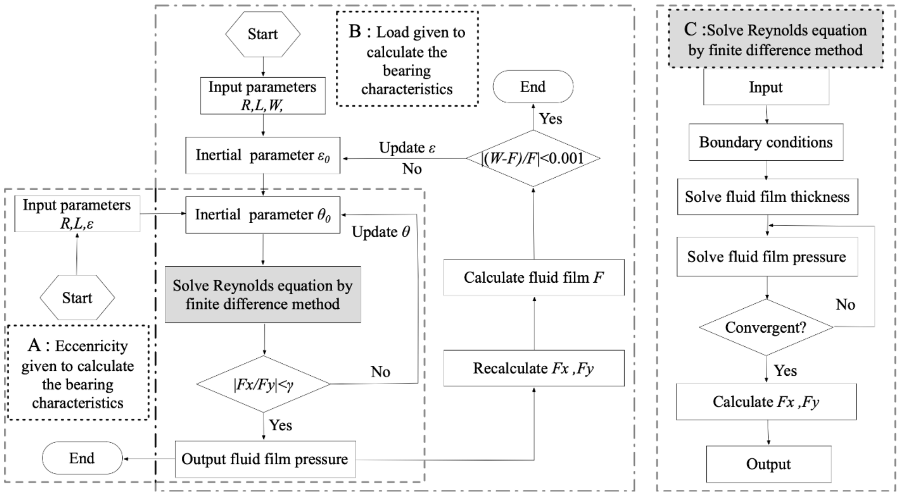

Figure 3. Flowchart for the calculation of the journal bearing.

In order to analyze the nonlinear dynamics characteristics of the rigid rotor-bearing system considering the journal disturbances, an algorithm is proposed. The algorithm is to solve the dynamic equations and the Reynolds equation simultaneously. In other words, the algorithm is to solve the second-order differential equations and the second-order partial differential equation simultaneously. The details are provided in Figure 4. The aim of this algorithm is to avoid the errors that come from two possible aspects: (1) when solving the stiffness and damping coefficients of the journal bearings, the linear hypothesis is used; (2) the linearized stiffness and damping coefficients are usually obtained by solving the perturbed Reynolds equation. However, the bearing performance considering the journal disturbance is obtained by solving the unsteady Reynolds equation. If the perturbation equation is used on this basis, the errors will be superimposed.

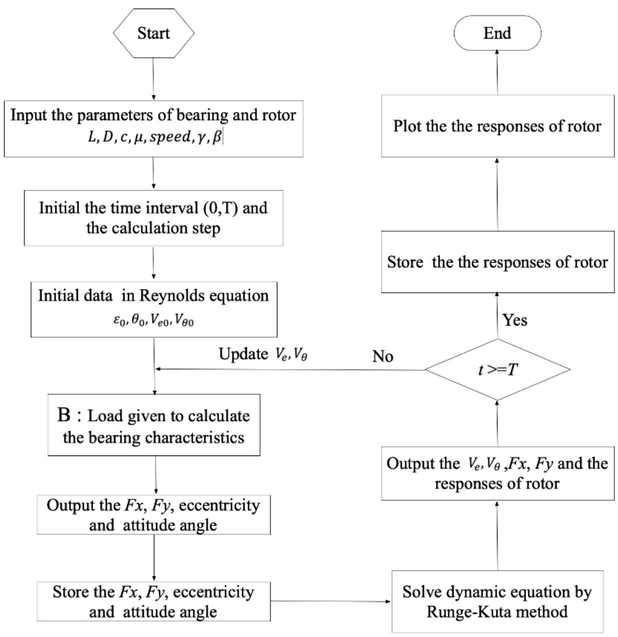

Figure 4. Flowchart of nonlinear analysis.

3. Results and Discussions

In this section, the characteristics of a bearing considering the journal disturbances are given. The nonlinear dynamic analysis of a rigid rotor-bearing system is also presented. The discussion of these results is given in detail.

3.1. The Characteristics of the Bearing

Table 1 gives the main parameters of a bearing considering the journal disturbances.

Table 1. Main parameters of the bearing and rotor.

	Parameters	Value
Bering	Diameter/mm	100.8
	Width/mm	100
	Clearance ratio	0.008
	Eccentricity	0.1~0.9
Rotor	γ/deg	0.01–0.04
	β/deg	0.01–0.08
	W/m·s-1	0–6
	Speed/rpm	3000
	Viscosity	0.009

Figure 5 shows the equilibrium position variation law with the variation in the bearing eccentricity. Figure 5a is the equilibrium position variation when the rotor rotates around the y-axis with a range of 0.01–0.04 degrees. The results indicate that the equilibrium position varies slightly when the eccentricity is less than 0.7 and changes greatly when the eccentricity is large. Figure 5b presents the equilibrium position variation law with the axial velocity of the journal. With the same eccentricity, the larger the axial velocity is, the lower the equilibrium position is. With the same axial velocity, the equilibrium position becomes lower with the increase in eccentricity. The variation law of the equilibrium position when the rotor rotates around the x-axis is given in Figure 5c. When the angle is small, the equilibrium position variation is not obvious, and the larger the angle is, the more obvious the variation. Figure 5d presents the equilibrium position variation law with the axial velocity of the journal when the angle with respect to the x-axis is constant. The results indicate that when the axial velocity varies, the eccentricity is larger, and there is a slighter effect on the equilibrium position variation.

The fluid film pressure distribution of the bearing is presented in Figure 6 under the parameters in Table 1. Figure 6a,b show the variation trends of the dimensionless pressure distribution of the bearing with the dimensionless bearing length when the rotor rotates around the y-axis and the x-axis, respectively. These two variation trends are similar. The results indicate that compared with the normal situation, the pressure distribution is not symmetric around the vertical line $\lambda = 0$. The maximum pressure becomes large with the increase in the angle. The position where the maximum pressure occurs also shifts as the angle increases. When the angle with respect to the y-axis varies from 0 to 0.04 degrees, the maximum pressure value increases by 10%, and the position where the maximum pressure occurs offsets by nearly 0.5 dimensionless bearing length. When the angle with respect to the x-axis varies from 0 to 0.04 degrees, the maximum pressure value increases by 7%, and the position where the maximum pressure occurs offsets by nearly 0.5 dimensionless bearing length. Figure 6c shows the dimensionless pressure distribution variation with the axial velocity when the angle with respect to the y-axis is constant. It can be concluded that the maximum pressure increases as the axial velocity increases, and it exhibits more than a 26% increase when the axial velocity varies from 0 to 8 m/s. However, the position where the maximum pressure occurs has little variation with respect to the axial velocity. Figure 6d presents the dimensionless pressure distribution variation with the length-to-radius (L/D) ratio of the bearing. As the L/D value increases, the maximum pressure value increases, and the position of the maximum pressure offsets. When the L/D value varies from 1 to 4, the maximum pressure value increases by nearly 90%, and the position where the maximum pressure occurs offsets to the right by nearly 60%.

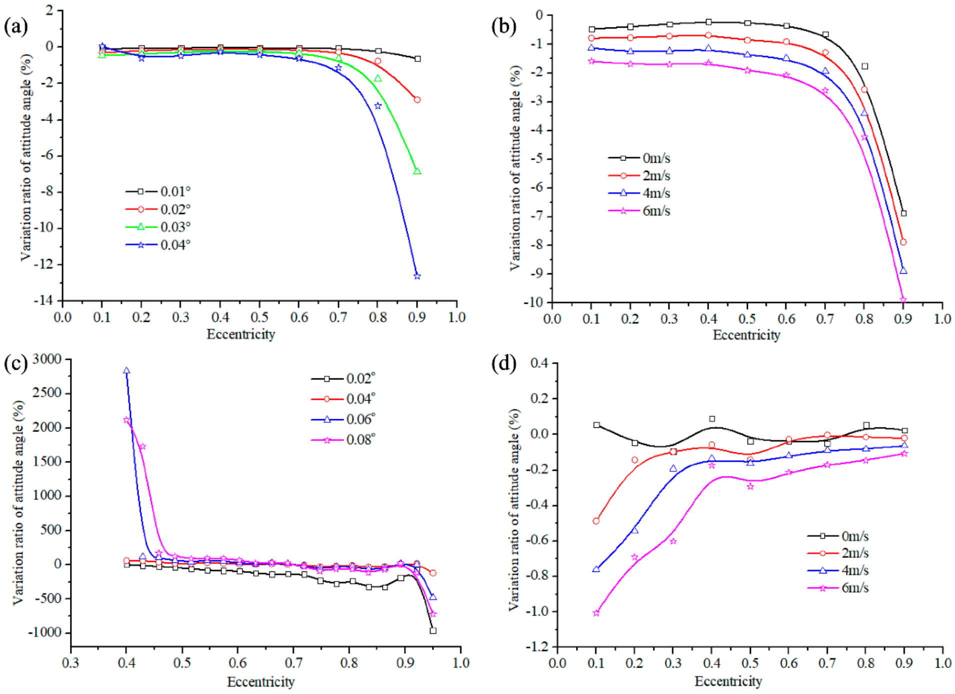

Figure 5. Equilibrium position variation: (**a**) is the equilibrium position variation with the rotor rotating about the *y*-axis; (**b**) is the equilibrium position variation law with the axial velocity; (**c**) is the equilibrium position with the rotor rotating about the *x*-axis; (**d**) is the equilibrium position variation law with the axial velocity of the journal when the angle with respect to the *x*-axis is constant.

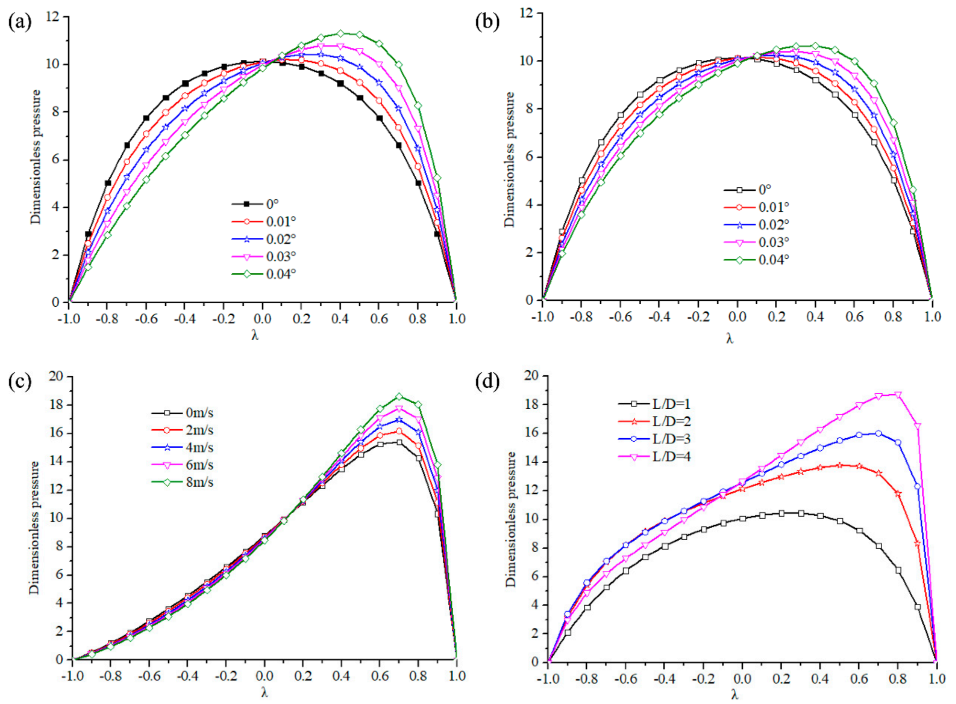

Figure 6. Fluid film pressure distribution: (**a**), (**b**) are pressure distributions of the bearing with the dimensionless bearing length when the rotor rotates around the *y*-axis and the *x*-axis, respectively; (**c**) is pressure distribution variation with the axial velocity; (**d**) is pressure distribution variation with the length-to-radius ratio.

The possible reasons for this are as follows: (1) when the rotor rotates around the *y*-axis, the fluid film thickness is a function of the *z*-coordinate, which results in the distribution variation of the fluid film pressure; (2) when the journal has a disturbance along the *z*-axis, the axial velocity will affect the hydrodynamic effects when the variation in the fluid film pressure distribution is considered, though the effect is slight when the rotating angle is small; and (3) the angle at which the rotor rotates should be limited to a certain range, especially when the eccentricity is much smaller or much larger. When the angle is too large, contact between the rotor and bearing might occur. Compared with the angle with respect to the *y*-axis, the angle with respect to the *x*-axis will affect the equilibrium position when the eccentricity is smaller, which may be a result of the fact that the attitude angle is generally larger when the eccentricity is smaller.

3.2. The Characteristics of a Rigid Rotor-Bearing System

Table 2 presents the main parameters of a rigid rotor-bearing system considering the journal disturbances.

Table 2. Main parameters of the rotor-bearing system.

	Parameters	Value
Bearing	Diameter/mm	100.8
	Width/mm	100
	Clearance ratio	0.008
	Eccentricity	0.75
Rotor	γ/deg	0.01–0.08
	β/deg	0.01–0.08
	W/m·s−1	0–6
	Speed/rpm	3000
	Unbalance mass/Kg·m	1.2
	Rotor mass/kg	400

Figure 7 shows the rotor responses and axis orbits under three working conditions: (a) different angles with respect to the *y*-axis; (b) different L/D values; and (3) different axial velocities. Because the influences on the angles concerning the x- and y-axes on the bearings are similar, the angles with respect to the *y*-axis are taken as an example.

Figure 7a shows that (1) as the angle with respect to the *y*-axis increases, the influence on the response of the x-direction is more obvious than that of the y-direction, though the most significant difference is the initial value in different conditions; (2) the influence on the response of the y-direction occurs on the positions with maximum vibration; the larger the angle value, the more obvious the variation; and (3) the axis orbit shape varies and the orbit offsets. When the angle value is 0.08, the orbit shape is obviously different compared with the shape at the small angle value.

The possible reason why these phenomena occurred in Figure 7a is that the fluid film dynamic characteristics vary due to the axis misalignment. The difference in the axis misalignment angle also causes equilibrium position variation, which results in the difference in the initial response value in both the x- and y-directions.

Figure 7b indicates that the influences on the responses and the axis orbit are much more obvious as the L/D values increase. The response in the x-direction is noticeably affected by the L/D value. The amplitude of the response increases as the L/D values increase, and the response contains multiple frequency components. Similarly, the response in the y-direction varies significantly with the change in the L/D values. The axis orbit shape varies greatly as the L/D values increase, which reflects the axis misalignment level.

These distinguishing features shown in Figure 7b may be caused by the different absolute displacements due to the divergence of the L/D values with the same misalignment angle. When the L/D value increases, the clearance between the journal and the bearing decreases rapidly. When the value reaches 5, contact and collision might occur.

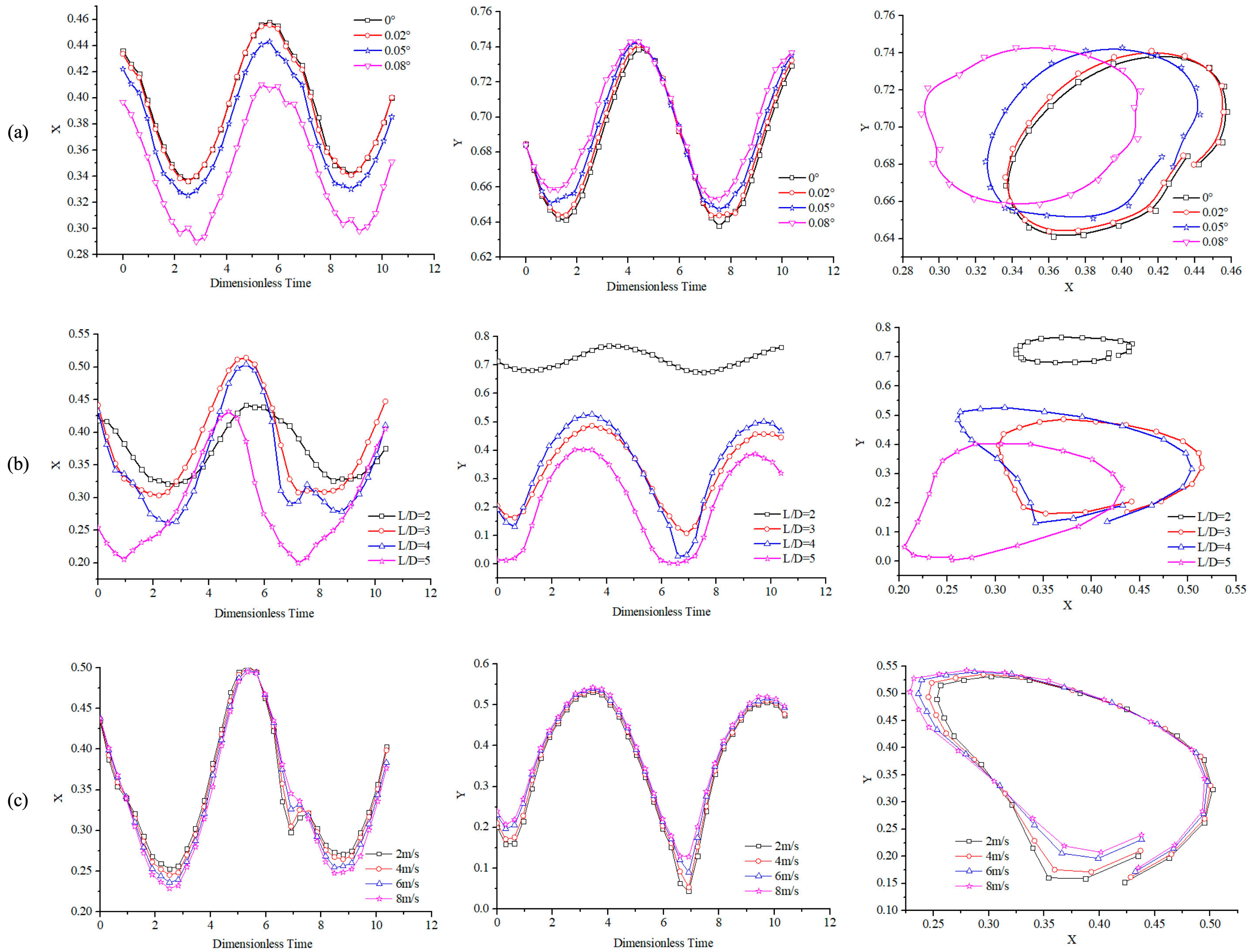

Figure 7. The responses and axis orbit: (**a**) is the axis orbit changing with the y-direction deflection angle of the rotor; (**b**) is the axis orbit changing with the L/D; (**c**) is the axis orbit changing with the axial velocity of the rotor.

The responses and axis orbit of the rotor-bearing system with the variation of the journal axial velocity are presented in Figure 7c. The response in the x-direction is affected less by the journal axial velocity, and the influences are mainly concentrated on the positions where the responses are large. There are fewer influences on the responses in the y-direction as the journal axial velocity increases, but the differences are obvious at the position where large responses occur. The axis orbit shape variation is not distinct, though the range of the axis orbit is significantly increased.

The possible reason for these features shown in Figure 7c is as follows. The hydrodynamic effect of the bearing is enhanced with the axial disturbance. The journal misalignment leads to a variation in the fluid film thickness distribution in the axial direction and the offset of the fluid film pressure distribution in the axial direction. When the axial disturbances and the misalignment work together, the variation trend is more obvious, which affects the capacity and dynamic characteristics of the bearing. Therefore, the variation range of the rotor equilibrium position increases.

4. Conclusions

A theoretical model using the dynamic equations for a journal bearing considering disturbances and a rigid rotor-bearing system is developed. A detailed algorithm that can simultaneously solve the rotor-dynamic equations and the Reynolds equation is proposed. The main conclusions are as follows:

(1) The disturbances in the circumferential and radial directions lead to the variation in the thickness distribution of the fluid film in the axial direction and the offset of the fluid film pressure distribution in the axial direction.
(2) The hydrodynamic effect of the bearing is enhanced with the axial disturbance. When disturbances in circumferential, radial, and axial directions work together, the variation trends of the fluid film thickness and pressure are more obvious.
(3) When the L/D value increases, the clearance between the journal and the bearing decreases rapidly.
(4) In future work, the efficiency of the algorithm needs to be improved according to different kinds of rotor-bearing systems.

Author Contributions: Conceptualization, Z.Z.; methodology, Z.Z. and P.Y.; software, Z.Z. and J.M.; validation, Z.Z., Q.L. and P.Y.; formal analysis, Z.Z and Q.L.; writing—original draft preparation, Z.Z. and J.M.; writing—review and editing, P.Y. and Q.L.; project administration, Z.Z.; funding acquisition, Z.Z. All authors have read and agreed to the published version of the manuscript.

Funding: This research was supported by the Scientific Research Program Funded by the Education Department of Shaanxi Provincial Government (Program No. 23JC014).

Institutional Review Board Statement: Not applicable.

Informed Consent Statement: Not applicable.

Data Availability Statement: The data presented in this study are available upon request from the corresponding author.

Conflicts of Interest: The authors declare no conflict of interest.

References

1. El-Butch, A.M.; Ashour, N.M. Transient analysis of misaligned elastic tilting-pad journal bearing. *Tribol. Int.* **2005**, *38*, 41–48. [CrossRef]
2. Rajput, A.K.; Sharma, S.C. Combined influence of geometric imperfections and misalignment of journal on the performance of four pocket hybrid journal bearing. *Tribol. Int.* **2016**, *97*, 59–70. [CrossRef]
3. Dal, A.; Karaçay, T. Effects of angular misalignment on the performance of rotor-bearing systems supported by externally pressurized air bearing. *Tribol. Int.* **2017**, *111*, 276–288. [CrossRef]
4. Meng, F.; Liu, R.; Qu, P.; Xu, G. Analysis of Misalignment Journal Bearings Considering the Turbulent Effects. In Proceedings of the 5th International Conference on Civil Engineering and Transportation 2015, Guangzhou, China, 28–29 November 2015.
5. Zhu, S.; Sun, J.; Li, B.; Zhao, X.; Wang, H.; Teng, Q.; Ren, Y.; Zhu, G. Research on Turbulent Lubrication of Misaligned Journal Bearing Considering the Axial Motion of Journal. *J. Tribol.* **2020**, *142*, 021802. [CrossRef]
6. Manser, B.; Belaidi, I.; Hamrani, A.; Khelladi, S.; Bakir, F. Performance of hydrodynamic journal bearing under the combined influence of textured surface and journal misalignment: A numerical survey. *Comptes Rendus Mécanique* **2019**, *347*, 141–165. [CrossRef]
7. Gu, C.; Meng, X.; Wang, S.; Ding, X. Modeling a Hydrodynamic Bearing with Provision for Misalignments and Textures. *J. Tribol.* **2020**, *142*, 041801. [CrossRef]
8. Jang, J.Y.; Khonsari, M.M. On the Behavior of Misaligned Journal Bearings Based on Mass-Conservative Thermohydrodynamic Analysis. *J. Tribol.* **2010**, *132*, 011702. [CrossRef]
9. Nikolakopoulos, P.G.; Papadopoulos, C.I.; Kaiktsis, L. Elastohydrodynamic analysis and Pareto optimization of intact, worn and misaligned journal bearings. *Meccanica* **2011**, *46*, 577–588. [CrossRef]
10. Li, B.; Sun, J.; Zhu, S.; Fu, Y.; Zhao, X.; Wang, H.; Teng, Q.; Ren, Y.; Li, Y.; Zhu, G. Thermohydrodynamic lubrication analysis of misaligned journal bearing considering the axial movement of journal. *Tribol. Int.* **2019**, *135*, 397–407. [CrossRef]
11. Xu, H.Y.; Yang, Y.; Ma, H.; Luo, Z.; Li, X.P.; Han, Q.K.; Wen, B.C. Vibration characteristics of bearing-rotor systems with inner ring dynamic misalignment. *Int. J. Mech. Sci.* **2022**, *230*, 107536. [CrossRef]
12. Sahu, K.; Sharma, S.C.; Ram, N. Misalignment and Surface Irregularities Effect in MR Fluid Journal Bearing. *Int. J. Mech. Sci.* **2022**, *221*, 107196. [CrossRef]
13. Elsayed, E.K.; Sayed, H.; El-Sayed, T.A. Analysis of Second-Order Thrust Bearing Coefficients Considering Misalignment Effect. *J. Vib. Eng. Technol.* **2023**. [CrossRef]
14. Guo, H.; Bao, J.Q.; Zhang, S.L.; Shi, M.H. Experimental and Numerical Study on Mixed Lubrication Performance of Journal Bearing Considering Misalignment and Thermal Effect. *Lubricants* **2022**, *10*, 262. [CrossRef]

15. Nikolakopoulos, P.G.; Papadopoulos, C.A. Dynamic Stability of Linear Misaligned Journal Bearings via Lyapunov's Direct Method©. *Tribol. Trans.* **1997**, *40*, 138–146. [CrossRef]
16. Nikolakopoulos, P.G.; Papadopoulos, C.A. Lyapunov's Stability of Nonlinear Misaligned Journal Bearings. *J. Eng. Gas Turbines Power.* **1995**, *117*, 576. [CrossRef]
17. Koondilogpiboon, N.; Inoue, T. Nonlinear Vibration Analysis of a Flexible Rotor Supported by a Journal Bearing Considering Journal Angular Motion. *J. Comput. Nonlinear Dyn.* **2020**, *15*, 091002. [CrossRef]
18. Wang, P.; Xu, H.; Ma, H.; Yang, Y.; Han, Q.; Wen, B.; Li, X. Nonlinear response of rotor system with bearing dynamic misalignment. *Mech. Based Des. Struct. Mach.* **2023**, 1–22. [CrossRef]
19. Han, Y.; Chan, C.; Wang, Z.; Shi, F.; Wang, J.; Wang, N.; Wang, Q.J. Effects of Shaft Axial Motion and Misalignment on the Lubrication Performance of Journal Bearings via a Fast Mixed EHL Computing Technology. *Tribol. Trans.* **2015**, *58*, 247–259. [CrossRef]
20. Li, B.; Sun, J.; Zhu, S.; Fu, Y.; Zhao, X.; Wang, H.; Teng, Q.; Ren, Y.; Li, Y.; Zhu, G. Effect of the axial movement of misaligned journal on the performance of hydrodynamic lubrication journal bearing with rough surface. *Mech. Ind.* **2019**, *20*, 402. [CrossRef]
21. Zhang, X.; Yin, Z.; Dong, Q. An experimental study of axial misalignment effect on seizure load of journal bearings. *Tribol. Int.* **2019**, *131*, 476–487. [CrossRef]
22. Mian, T.; Choudhary, A.; Fatima, S. Multi-Sensor Fault Diagnosis for Misalignment and Unbalance Detection Using Machine Learning. *IEEE Trans. Ind. Appl.* **2023**, *59*, 5749–5759. [CrossRef]
23. Xu, Y.J.; Liu, J.Z.; Wan, Z.; Zhang, D.H.; Jiang, D. Rotor Fault Diagnosis Using Domain-Adversarial Neural Network with Time-Frequency Analysis. *Machines* **2022**, *10*, 610. [CrossRef]
24. Zhang, J.; Zhao, H.; Zou, D.; Ta, N.; Rao, Z. Comparison study of misalignment effect along two perpendicular directions on the stability of rigid rotor-aerostatic journal bearing system. *Proc. Inst. Mech. Eng. Part J J. Eng. Tribol.* **2020**, *234*, 1618–1634. [CrossRef]